Inelastic electronic light scattering in superconducting and normal metals with impurities

L. A. Falkovsky

L. D. Landau Institute of Theoretical Physics, Russian Academy of Sciences
(Submitted 28 September 1992)
Zh. Eksp. Teor. Fiz. **103**, 666–679 (February 1993)

Effects of impurities and Coulomb screening on the Raman scattering of light by electrons in normal and superconducting metals are considered. In contrast to scattering in pure metals, the effect of Coulomb screening is unimportant. Impurities leave unchanged the threshold of the frequency shift but have an appreciable influence on the intensity of the scattering both near the threshold and at higher frequencies.

1. INTRODUCTION

Electronic Raman light scattering continues to attract the attention of both theorists and experimentalists because—as the original theory suggests[1,2]—it gives a direct measure of the superconducting energy gap. As far as conventional superconductors are concerned, the first scattering experiments[3,4] have confirmed this prediction: the threshold based gap is identical to that from tunnel experiments.

High-temperature superconductors present a more complicated situation (see Ref. 5 for a review; also note Refs. 6 and 7). Scattering below the expected threshold has been experimentally observed, as well as a polarization dependence of the position of the cross section maximum. The former phenomenon may be explained by the energy gap going to zero in some regions either of the Fermi surface[8] or of the sample. The polarization dependence has recently been accounted for[9] by modeling a superconductor as a system of alternate normal and superconducting layers.

On the other hand, analysis of anisotropic superconductors shows the theory to be inadequate:[2,9] at large frequency shifts the scattering cross section tends to zero instead of approaching the value in the normal metal as it obviously should. The present study shows that this difficulty may be eliminated by introducing the effects of impurities.

So far, the effects of impurities on the scattering have only been considered for a normal metal. For an isotropic metal, it has been found[10] that scattering appears only in second order in the momentum transfer q and that it is due to diffusion creation processes. For an anisotropic metal,[11] a nontrivial result is obtained even in zeroth order in q. The important point here is that in a dirty metal the scattering cross section only starts to decrease when $\omega_0 \gg \tau^{-1}$, whereas in a pure metal this occurs at far lower values of the shift frequency $\omega_0 = \omega_i - \omega_s$ (ω_i and ω_s are the frequencies of the incident and scattered light, respectively, and τ is the electron-impurity collision frequency). The scattering analysis of Ref. 11 neglects Coulomb screening effects whose crucial importance for a pure metal was demonstrated in Ref. 12.

In the present study the effects of impurities and Coulomb screening on the Raman scattering in a normal metal and a superconductor are considered. The impurity potential is taken to have a short range and hence to be independent of the scattering angle in momentum space. This assumption makes the problem tractable and is physically justified by the fact that the screening of an impurity potential in a metal typically occurs at interatomic distances.

2. RAMAN SCATTERING IN A NORMAL METAL

We begin by calculating the electron loop diagram responsible for the inelastic light scattering in a metal. In Fig. 1 the effect of impurities on the scattering is represented by a typical diagram having an arbitrary number of dashed impurity lines. A vertex in the diagram is associated with the momentum-dependent factor $\gamma(\mathbf{p}) = e_\alpha^{(i)} m_{\alpha\beta}{}^{-1} e_\beta^{(s)}$, where $\mathbf{e}_\alpha^{(i)}$ and $\mathbf{e}_\alpha^{(s)}$ are the polarization vectors of the incident and scattered light, respectively, and $m_{\alpha\beta}^{-1}$ is the (*generalized*) inverse effective-mass tensor which we assume to take account of the interband transitions resonant at the frequencies ω_i and ω_s of the incident and scattering light.

A series of such diagrams is summed using the vertex function equation

$$\Pi_\gamma(p_+, p_-) = G(p_+)G(p_-) \times \left(\gamma(\mathbf{p}) + \frac{n}{(2\pi)^3}\int |u(\mathbf{p}-\mathbf{p}^1)|^2 \Pi_\gamma(p_+^1, p_-^1) d^3p^1\right), \tag{1}$$

where $G(p) = [i\omega - \xi + (1/2\tau)(\omega/|\omega|)]^{-1}$ is the electron Green's function dependent on the four-momentum $p = (\mathbf{p}, \omega)$; $p_\pm = p \pm q/2$, where $q = (\mathbf{q}, q_0)$ is the four-momentum transfer; n is the impurity concentration; $u(\mathbf{p}-\mathbf{p}^1)$ the amplitude of impurity scattering; τ^{-1} the collision frequency.

In the approximation where the amplitude is independent of the scattering angle, $u(\mathbf{p}-\mathbf{p}^1) = u_0$, and Eq. (1) is easily solved to give

$$\Pi_\gamma(p_+, p_-) = G(p_+)G(p_-)\left(\gamma(\mathbf{p}) + \frac{I_\gamma(\mathbf{q}, q_0)}{1 - I(\mathbf{q}, q_0)}\right), \tag{2}$$

where

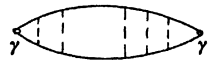

FIG. 1. Electron correlation function. Solid lines: Green's functions; dashed lines: impurity scattering; γ: electron–photon vertex.

 1063-7761/93/020331-06$10.00

$$I_\gamma(\mathbf{q}, q_0) = \frac{|u_0|^2 n}{(2\pi)^3}\int d^3p\gamma(\mathbf{p})G(p_+)G(p_-), \tag{3}$$

and the quantity I differs from I_γ in not having γ under the integral. We now write $\xi(\mathbf{p}_\pm) = \xi(\mathbf{p}) \pm \mathbf{vq}/2$ and integrate over ξ using

$$\frac{2d^3p}{(2\pi)^3} = \frac{\nu}{4\pi}d\xi do,$$

where ν is the density of states and do is the solid angle element on the Fermi surface. We find

$$I_\gamma(\mathbf{q}, q_0) = \frac{i}{4\pi\tau}\int \frac{\gamma(\mathbf{p})do}{iq_0 - \mathbf{vq} + i/\tau} \quad \text{for} \quad \omega^2 < q_0^2/4$$

and (4)

$$I_\gamma(\mathbf{q}, q_0) = 0 \quad \text{for} \quad \omega^2 > q_0^2/4,$$

where $\tau^{-1} = \pi\nu n|u_0|^2$ is the collision frequency.

The scattering cross section is determined by the imaginary part of the retarded function $K^R_{\gamma^2}(\mathbf{q}, \omega_0)$ obtained from the integral of the vertex part,

$$K_{\gamma^2}(\mathbf{q}, q_0) = 2T\sum_\omega \int \frac{d^3p}{(2\pi)^3}\gamma(\mathbf{p})\Pi_\gamma(p_+, p_-) \tag{5}$$

by analytically continuing it to the real frequencies $\omega_0 = iq_0$ so that the resulting function has no singularities in the upper half ω_0 plane. For a normal metal, we will see below that it suffices to formally replace q_0 by $-i\omega$ in $K^R_{\gamma^2}(\mathbf{q}, q_0)$ in order to obtain a retarded function with the required analytical properties.

The calculation is complicated by the fact that we must first sum over the frequencies $\omega = (2n+1)\pi T$ in (5). Since it is easier to begin with the ξ integration—and noting the slow convergence of (5)—let us modify the integrand by adding and subtracting the corresponding value calculated in the $\tau\to\infty$ limit. For a pure metal, $K^R_{\gamma^2}(\mathbf{q}, \omega_0)$ is readily calculated to give

$$\lim_{\tau\to\infty} K^R_{\gamma^2}(\mathbf{q}, \omega_0) = \frac{\nu}{4\pi}\int do\gamma^2(p)\frac{vq}{-vq + \omega_0 + io}. \tag{6}$$

Now we may change the order of summation and integration when evaluating the remainder. We find

$$K^R_{\gamma^2}(\mathbf{q}, \omega_0) = \frac{\nu}{4\pi}\int do\,\gamma(\mathbf{p})$$

$$\times\left[-\gamma(\mathbf{p}) + \frac{\omega_0}{\omega_0 - \mathbf{vq} + i/\tau}\left(\gamma(\mathbf{p}) + \frac{I_\gamma(\mathbf{q}, -i\omega_0)}{1 - I(\mathbf{q}, -i\omega_0)}\right)\right], \tag{7}$$

where I_γ and I should be taken as given in (4) for $\omega^2 < q_0^2/4$.

The characteristic value of q will now be obtained by integrating expression (7) multiplied by a factor that depends on the electric field distribution in the metal. For a dirty metal, the dominant role is played by the small values of the parameter $\mathbf{vq}/(\omega_0 + i/\tau)$. For $\mathbf{q} = 0$,

$$I_\gamma(0, -i\omega_0) = \frac{i/\tau}{\omega_0 + i/\tau}\bar{\gamma}, \tag{8}$$

the bar denoting averaging over the angle over the Fermi surface. Substituting (8) into (7) and taking the imaginary part we obtain

$$-\mathrm{Im}\, K^R_{\gamma^2}(0, \omega_0) = \nu\frac{\omega_0\tau^{-1}}{\omega_0^2 + \tau^{-2}}\left(\bar{\gamma^2} - \bar{\gamma}^2\right). \tag{9}$$

Note that the frequency dependence of (9) agrees with that obtained in Ref. 11; in the isotropic case this expression vanishes in accordance with Ref. 10.

As we shall see, at low frequencies ω_0 the following approximation in q is useful. Turning to expression (4), let us expand its integrand to second order in $\mathbf{vq}/(\omega_0 + i/\tau)$ (we note that the first-order term vanishes because of the $\mathbf{v}\to -\mathbf{v}$ symmetry). Integrating over the angles then yields

$$I_\gamma(\mathbf{q}, -i\omega_0) = \frac{i/\tau}{\omega_0 + i/\tau}\left[\bar{\gamma} + \frac{v_i v_k\gamma}{(\omega_0 + i/\tau)^2}q_i q_k\right]. \tag{10}$$

Substituting (10) into (7) and separating the imaginary part we have

$$-\mathrm{Im}\, K^R_{\gamma^2}(q, \omega_0) = \frac{\nu\omega_0\tau^{-1}}{\omega_0^2 + z^2\tau^{-2}}\left[\frac{\omega_0^2 + z/\tau^2}{\omega_0^2 + \tau^{-2}}\left(\bar{\gamma^2} - \bar{\gamma}^2\right) + z\bar{\gamma^2}\right], \tag{11}$$

where $z = q_i q_k\,\overline{v_i v_k}\tau^2$ for $\omega_0\tau \ll 1$ and $z = -q_i q_k\,\overline{v_i v_k}\tau^2$ for $\omega_0\tau \gg 1$. Note that the pole of the first factor in (11) describes the creation of diffusions.

It should be emphasized that Eq. (11) is obtained by expanding in z: We have neglected the z terms as small compared to unity but retained the terms of order $z/(\omega_0\tau)^2$ and $(z/\omega_0\tau)^2$ because $\omega_0\tau$ may be small.

3. EFFECT OF COULOMB SCREENING ON THE SCATTERING IN A DIRTY METAL

To account for the Coulomb interaction of electrons, the loop for the series of diagrams shown in Fig. 2 needs to be calculated. A wavy line in the figure describes the electron–electron potential $V = 4\pi e^2/q_i q_j \varepsilon^0_{ij}$ with screening accounted for by the dielectric function ε^0_{ij} due to the valence electrons (the conduction-electron contribution is represented by the series of Fig. 2).

Performing the summation we find

$$\mathcal{K}_{\gamma^2} = K_{\gamma^2} + K_\gamma V K_\gamma + K_\gamma V K V K_\gamma + \ldots$$

$$= K_{\gamma^2} + K_\gamma\frac{V}{1 - KV}K_\gamma, \tag{12}$$

where K_{γ^2} is the loop diagram (7) accounting for the effect

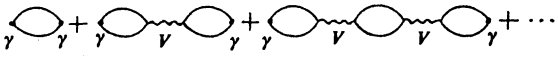

FIG. 2. The sum of Coulomb diagrams. Wavy line: electron–electron interaction potential.

of impurities in the absence of the Coulomb interaction, K_γ is the integral of the vertex function (2),

$$K_\gamma = 2T\sum_\omega \int \frac{d^3p}{(2\pi)^3}\Pi_\gamma(p_+, p_-), \tag{13}$$

and K is obtained from K_γ by replacing γ by unity.

Using Eqs. (2)–(4), it is found that following the angle integration, the zeroth-order term in $\mathbf{q}$ disappears from K_γ and the remaining expression is proportional to q^2:

$$K_\gamma^R = \frac{\nu q_i q_k}{(\omega + i/\tau)^3}\left(\omega\overline{\gamma v_i v_k} + \frac{i}{\tau}\bar{\gamma}\,\overline{v_i v_k}\right)\left(1 + \frac{i/\tau}{\omega + i\overline{v_j v_l} q_j q_l \tau}\right). \tag{14}$$

Equation (12) shows the importance of the quantity KV. Using (14) we find that for the dominant region $\omega_0 < \tau^{-1}$

$$KV \sim \frac{\tau v^2}{\omega_0} r_D^{-2} \geq \left(\frac{l}{r_D}\right)^2, \tag{15}$$

where $r_D \sim (4\pi\nu e^2/\varepsilon^0)^{-1/2}$ is the Debye radius and $l = \tau v$ the mean free path. Since the latter is usually much greater than the former, we may neglect unity in comparison with KV in Eq. (12) to obtain

$$\mathcal{K}_{\gamma^2} = K_{\gamma^2} - K_{\gamma^2}/K. \tag{16}$$

By (14) and (15), the ratio K_γ/K is found to be

$$K_\gamma^R/K^R = q_i q_k(\omega\overline{\gamma v_i v_k} + \frac{i}{\tau}\bar{\gamma}\,\overline{v_i v_k})/q_j q_l \overline{v_j v_l}(\omega + i/\tau). \tag{17}$$

Using (11), (16), and (17) one finds that for $\omega_0 < \tau^{-1}$

$$-\mathrm{Im}\,\mathcal{K}_{\gamma^2}^R = \frac{\nu\omega_0/\tau}{\omega_0^2 + z^2\tau^{-2}}\left[(\omega_0\tau)^2 + 2z\right]\left(\overline{\gamma^2} - \bar{\gamma}^2\right), \tag{18}$$

where $z = q_i q_k\,\overline{v_i v_k}\tau^2$.

By comparing Eq. (18) with Eq. (11) for $\omega_0 < \tau^{-1}$, we see that it is only the last term which has changed: if γ is independent of the angle, Im $\mathcal{K}_{\gamma^2}^R$ vanishes when the Coulomb screening is taken into account. The frequency dependence of Im $\mathcal{K}_{\gamma^2}^R$—and hence of the cross section—remains unchanged.

4. EFFECTIVE SCATTERING CROSS SECTION IN A DIRTY NORMAL METAL

It is essential for scattering cross section calculations that the incident and scattered radiation propagate in a medium. In the optical range, we may characterize the medium by its permittivity ε and refraction and attenuation coefficients ($n_i + i\varkappa_\alpha = \sqrt{\varepsilon_\alpha}$, $\alpha = i, s$) referred to a given frequency of the (incident or scattered) light. We consider the frequency shift $\omega_0 = \omega_i - \omega_s$ to be small compared to ω_i and ω_s, but we retain the dependence of both n and $\varkappa$ on the light polarization direction (assumed to coincide with one of the principal axes of the ε tensor). A particularly simple cross section formula is obtained for the incident and scattered light propagating normal to the plane surface of the metal:[1,13]

$$\frac{d\sigma}{d\omega_s do_s} = \left(\frac{2e^2}{\hbar c^2\pi}\right)^2 \frac{J}{1 - \exp(-\hbar\omega/kT)}$$

$$\times\left[\left(1 + n_s\right)^2 + \varkappa_s^2\right]^{-1}\left[\left(1 + n_i\right)^2 + \varkappa_i^2\right]^{-1},$$

$$J = -\frac{1}{\pi}\int_0^\infty dq|f(q)|^2\,\mathrm{Im}\,K_{\gamma^2}^R(q, \omega_0), \tag{19}$$

where $|f(q)|^2$ depends on the propagation characteristics of the electric field in the metal. For example,

$$|f(q)|^2$$

$$= \left\{\left[\frac{\omega_i}{c}(n_i + n_s) - q\right]^2 + \frac{\omega_i^2}{c^2}(\varkappa_i + \varkappa_s)^2\right\}^{-1} \quad \text{for } \varkappa \ll n, \tag{20}$$

$$|f(q)|^2$$

$$= 4\frac{\omega_i^2}{c^2}(\varkappa_i + \varkappa_s)^2\left[q^2 + \frac{\omega_i^2}{c^2}(\varkappa_i + \varkappa_s)^2\right]^{-2} \quad \text{for } \varkappa \gg n. \tag{21}$$

Note that Eq. (20) implies that the attenuation of light in the metal is small and that the assumed "back-scattering" geometry results in the momentum transfer being the sum of the momenta of the absorbed and emitted photons. Clearly this equation yields a greater scattering cross section than does Eq. (21): note the small quantity $\varkappa$ which appears in the denominator following the q integration. We thus restrict ourselves to the more interesting case of Eq. (20).

In order to evaluate the integral (19), we note that the spread (in q) of the maximum of the function (18) is estimated by the inequality $z < \omega_0\tau$, i.e., $q \sim z^{1/2}/v\tau \lesssim (1/v)\sqrt{\omega_0\tau}$. If $(1/v)(\omega_0/\tau)^{1/2} \gg \omega_i(n_i + n_s)/c$, then the sharp maximum of the function (20) is superimposed on the relatively broad maximum of (18) [or (9)] and the integral (19) becomes

$$J = \frac{\nu(\overline{\gamma^2} - \bar{\gamma}^2)}{\omega_0\tau(\omega_0^2 + \tau^{-2})}$$

$$\times\left[\omega_0^2 + 2\bar{v}_z^2\left(\frac{\omega_i}{c}\right)^2\left(n_i + n_s\right)^2\right]\frac{c}{\omega_i(\varkappa_i + \varkappa_s)}, \tag{22}$$

where v_z denotes the projection of the electron velocity on the surface normal.

If $(\omega_0/\tau)^{1/2}/v \ll \omega_i(n_i + n_s)/c$, then the maxima of the functions (18) and (20) do not overlap one another and their contributions must be calculated separately. We have

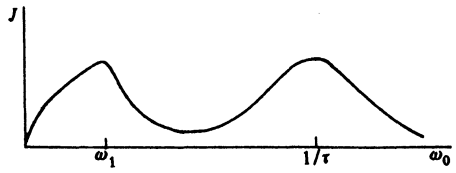

FIG. 3. Scattering cross section versus shift frequency for low temperatures $kT \ll \hbar\omega_0$; $\omega_1 \sim \overline{v_z^2}[\omega_i(n_i+n_s)/c]^2$.

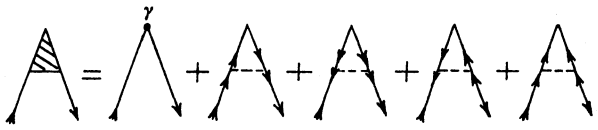

FIG. 4. Equation for the vertex function $\Pi^{(1)}$.

$$J = \nu(\overline{\gamma^2} - \bar{\gamma}^2)\left(\frac{\omega_0}{\tau\overline{v_z^2}}\right)^{1/2}\frac{c^2}{\omega_i^2(n_i+n_s)^2}$$

$$\times\left[\frac{1}{\sqrt{2}} + 2\left(\frac{\omega_0}{\tau\overline{v_z^2}}\right)^{1/2}\frac{c}{\omega_i(\varkappa_i+\varkappa_s)}\right]. \tag{23}$$

A plot of J versus ω_0 is shown in Fig. 3. For the low frequencies

$$\omega_0 < \tau\overline{v_z^2}[\omega_i(\varkappa_i+\varkappa_s)/c]^2,$$

the cross section exhibits the square root behavior corresponding to the first term in (23). Next follows the region

$$\tau\overline{v_z^2}[\omega_i(\varkappa_i+\varkappa_s)/c]^2 \ll \omega_0 \ll \tau\overline{v_z^2}[\omega_i(n_i+n_s)/c]^2$$

which shows a linear dependence corresponding to the second term in (23), and then we come to a maximum whose position corresponds to the creation of a diffusion with a momentum equal to the sum of the momenta of the absorbed and emitted photons:

$$\omega_0 = \omega_1 \sim \tau\overline{v_z^2}[\omega_i(n_i+n_s)/c]^2,$$

Following the maximum the cross section starts to decrease [the second term in the bracket in (22), $\omega_0 \ll \tau^{-1}$] and reaches a minimum at

$$\omega_0 \sim (\overline{v_z^2})^{1/2}\omega_i(n_i+n_s)/c.$$

After this the dominant role is played by the first term in (22), and we thus arrive at a second maximum, located at $\omega_0 = \tau^{-1}$ and having the same height as the first.

At nonzero temperatures, the exponential factor in (19) should also be taken into account. Note that for $T > \omega_1$ the low-frequency maximum is absent. It should be emphasized that the conditions for which the above formulas are obtained are that the mean free path is small,

$$l\omega_i(n_i+n_s)/c \ll 1, \tag{24}$$

and that both the incident and scattered light experience a relatively weak attenuation in the metal ($\varkappa_i \ll n_i$).

5. SCATTERING IN A DIRTY SUPERCONDUCTOR

Our analysis is limited to the most interesting case, that for which $v\omega_i(n_i+n_s)/c \ll \Delta$, Δ being the gap, and we again assume (24) to hold. We allow the effective mass to be anisotropic (noting that it determines the vertex γ), but we neglect the anisotropy of the energy gap Δ. In this approximation, it is known[2] that the loop diagrams with superconducting vertices contribute little—in much the same way as the Coulomb interaction in a normal metal turns out to be small: see the second term in (22) for $\omega_0 \geqslant 2\Delta$. We may therefore restrict ourselves to the main loop diagram as shown in Fig. 1. This time, however, the anomalous Green's function F enters the analysis and we therefore have four types of vertex diagrams to consider. Instead of (1) we have

$$\Pi^{(i)} = \Pi_0^{(i)} + a_{ik}\Lambda^{(k)}. \tag{25}$$

One of equations (25) is shown in Fig. 4.

To zeroth order in the impurity scattering, the vertex diagrams are

$$\Pi_0^{(1)}(p_+, p_-) = \gamma(\mathbf{p})[G(p_+)G(p_-) - F(p_+)F^+(p_-)],$$

$$\Pi_0^{(2)}(p_+, p_-) = \gamma(\mathbf{p})[G(p_+)F(p_-) + F(p_+)G(-p_-)],$$

$$\Pi_0^{(3)}(p_+, p_-) = \gamma(\mathbf{p})[G(-p_+)G(-p_-) - F^+(p_+)F(p_-)], \tag{26}$$

$$\Pi_0^{(4)}(p_+, p_-) = \gamma(\mathbf{p})[-F^+(p_+)G(p_-) - G(-p_+)F^+(p_-)].$$

The coefficients a_{ik} form the matrix

$$\begin{pmatrix} G(p_+)G(p_-) & -G(p_+)F^+(p_-) & -F(p_+)F^+(p_-) & F(p_+)G(p_-) \\ G(p_+)F(p_-) & G(p_+)G(-p_-) & F(p_+)G(-p_-) & F(p_+)F(p_-) \\ -F^+(p_+)F(p_-) & -F^+(p_+)G(-p_-) & G(-p_+)G(-p_-) & G(-p_+)F(p_-) \\ -F^+(p_+)G(p_-) & F^+(p_+)F^+(p_-) & -G(-p_+)F^+(p_-) & G(-p_+)G(p_-) \end{pmatrix}, \tag{27}$$

and the quantities $\Lambda^{(1)}$ are obtained by integration,

$$\Lambda^{(1)} = \frac{n}{(2\pi)^3}\int |u(\mathbf{p}-\mathbf{p}^1)|^2\Pi^{(1)}(p_+^1, p_-^1)d^3p^1. \tag{28}$$

The condition (24) enables one to restrict the analysis to the $\mathbf{q}\to 0$ limit, the $\pm$ signs then only indicating the shifts in the frequency variable, $\omega_\pm = \omega \pm q_0/2$. In the case of impurity scattering the Green's functions are[14]

$$G = -\frac{i\omega\eta + \xi}{\xi^2 + \eta^2(\Delta^2+\omega^2)}, \quad F = F^+ = \frac{\Delta\eta}{\xi^2 + \eta^2(\Delta^2+\omega^2)},$$

where $\eta = 1 + 1/2\tau\sqrt{\omega^2 + \Delta^2}$.

If the scattering amplitude is taken to be independent of the angle, then $u(\mathbf{p} - \mathbf{p}^1) = u_0$ and Eq. (25) assumes the algebraic form

$$\Lambda^{(i)} = \Lambda_0^{(i)} + I_{ik}\Lambda^{(k)}, \tag{29}$$

where

$$I_{ik} = \frac{|u_0|^2}{(2\pi)^3}\int a_{ik}d^3p. \tag{30}$$

Now the odd powers of ξ disappear when the products of the Green's functions are integrated over ξ. Hence

$$\Lambda_0^{(1)} = \Lambda_0^{(3)} \text{ and } \Lambda_0^{(2)} = \Lambda_0^{(4)}, \tag{31}$$

and from the symmetry of the integrals I_{ik} it follows that the expressions (31) relate the exact $\Lambda^{(i)}$ as well.

Using Eqs. (26)–(28) and (30), we evaluate the quantities $\Delta_0^{(i)}$ and I_{ik} and solve Eqs. (29) to obtain

$$\Lambda^{(1)} = \frac{\bar{\gamma}}{2\tau}\frac{s_+s_- - \omega_+\omega_- - \Delta^2}{s_+s_-(s_+ + s_-)},$$

$$\Lambda^{(2)} = -\frac{\bar{\gamma}i}{2\tau}\frac{q_0\Delta}{s_+s_-(s_+ + s_-)}, \tag{32}$$

where $s_\pm = \sqrt{(\omega \pm q_0/2) + \Delta^2}$.

The Raman scattering cross section is calculated by performing an analytical continuation to real frequencies $\omega_0 = iq_0$ of the correlation function

$$K(q_0) = 2T\sum_\omega\int\frac{d^3p}{(2\pi)^3}\gamma(\mathrm{p})\Pi^{(1)}(p_+, p_-), \tag{33}$$

which may be rewritten using (25) as

$$K(q_0) = 2T\sum_\omega\int\frac{d^3p}{(2\pi)^3}\gamma(\mathrm{p})$$

$$\times\left\{\left(\gamma(\mathrm{p}) + \Lambda^{(1)}\right)[G(p_+)G(p_-) - F(p_+)F^+(p_-)]\right.$$

$$\left. + \Lambda^{(2)}[-G(p_+)F^+(p_-) + F(p_+)G(p_-)]\right\}. \tag{34}$$

The integrand of this expression [which we denote by $f(q_0, \omega, \xi)$] must first be summed over ω and then integrated over ξ. It is convenient to interchange these processes, however. For this purpose, let us make (34) convergent by adding and subtracting the term $f(0, \omega, \xi)$ in the integrand. Summing and integrating $f(0, \omega, \xi)$ then yields a pure real expression of no importance to the problem, whereas the difference $f(q_0, \omega, \xi) - f(0, \omega, \xi)$ may be summed and integrated in either order.

Integrating over ξ we find

$$\int d\xi\left(G(p_+)G(p_-) - F(p_+)F^+(p_-)\right) = \pi\frac{s_+s_- - \omega_+\omega_- - \Delta^2}{s_+s_-(s_+ + s_- + 1/\tau)},$$

$$\int d\xi\left(-G(p_+)F^+(p_-) + F(p_+)G(p_-)\right) \tag{35}$$

$$= i\pi\frac{q_0\Delta}{s_+s_-(s_+ + s_- + 1/\tau)}.$$

Substituting (35) into (34) yields

$$K(q_0) = \pi\nu T\sum_\omega\frac{s_+s_- - \omega_+\omega_- - \Delta^2}{s_+s_-(s_+ + s_- + 1/\tau)}\left(\bar{\gamma}^2 + \frac{\bar{\gamma}^2}{\tau(s_+ + s_-)}\right). \tag{36}$$

We proceed by shifting the summation variable according to $\omega \to \omega - q_0/2$ and replacing the sum by the integral

$$T\sum_\omega \ldots = \frac{i}{4\pi}\int d\omega\ \mathrm{tg}\frac{\omega}{2T}\ldots$$

over a contour enclosing the real axis. The analytical continuation of the integral is performed using the procedure given in Ref. 14. Separating the imaginary part we find

$$-\mathrm{Im}\,K^R(\omega_0) = \frac{\nu}{2\tau}(\bar{\gamma}^2 - \bar{\gamma}^2)\left\{\theta(\omega_0 - 2\Delta)\int_{\Delta-\omega_0}^{-\Delta} d\omega\ \mathrm{th}\frac{\omega}{2T}f(\omega, \omega_0)\right.$$

$$\left. + \int_\Delta^\infty d\omega\left(\mathrm{th}\frac{\omega_0 + \omega}{2T} - \mathrm{th}\frac{\omega}{2T}\right)f(\omega, \omega_0)\right\}, \tag{37}$$

where

$$f(\omega, \omega_0) = \frac{1 + [\omega(\omega + \omega_0) - \Delta^2]/ss_+}{(s - s_+)^2 + \tau^{-2}}$$

$$- \frac{1 - [\omega(\omega + \omega_0) - \Delta^2]/ss_+}{(s + s_+)^2 + \tau^{-2}}, \tag{38}$$

$$s = \sqrt{\omega^2 - \Delta^2}, \quad s_+ = \sqrt{(\omega + \omega_0)^2 - \Delta^2}.$$

In Eq. (37) the second term describes the light scattering due to thermal excitations above the gap; this term decreases exponentially for $T \ll \Delta$.

The first term in (37) relates to across-the-gap excitations and shows the threshold $\omega_0 = 2\Delta$ is not altered by impurities. For $T = 0$ this is the only term present, and if we change variables to $x = \omega_0 - 2\Delta$, $\omega = \Delta - xt$, it becomes

$$-\mathrm{Im}\,K^R = \frac{\nu}{2\tau}(\bar{\gamma}^2 - \bar{\gamma}^2)\,\theta(x)x\int_0^1 dt\,f(x, t), \tag{39}$$

where

$$f(x, t) = (1 + z)$$

$$\times\left\{\left[\sqrt{xt(2\Delta + xt)} + \sqrt{x(1 - t)[2\Delta + x(1 - t)]}\right]^2 + \tau^{-2}\right\}^{-1}$$

$$- (1 - z)\left\{\left[\sqrt{xt(2\Delta + xt)} - \sqrt{x(1 - t)[2\Delta + x(1 - t)]}\right]^2 + \tau^{-2}\right\}^{-1},$$

$$z = \frac{2\Delta^2 + \Delta x + x^2t(1 - t)}{x\{t(1 - t)(2\Delta + xt)[2\Delta + x(1 - t)]\}^{1/2}}.$$

In the vicinity of the threshold frequency ($x \to 0$), (39) yields

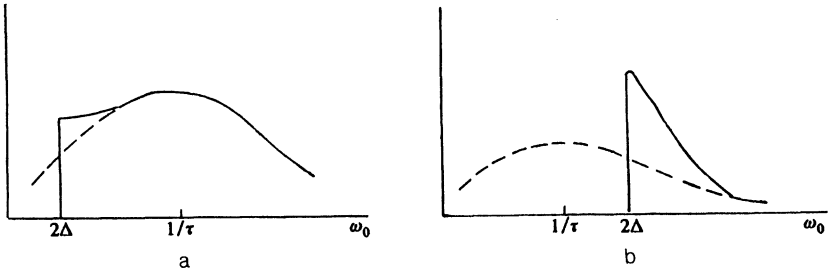

FIG. 5. Scattering cross section versus shift frequency in a superconductor at low temperatures $kT \ll \Delta$. The dashed line corresponds to a normal metal. (a): relatively pure superconductor $2\Delta \ll \tau^{-1}$; (b): dirty superconductor $2\Delta \gg \tau^{-1}$.

$$-\mathrm{Im}\, K^R = \nu(\overline{\gamma^2} - \bar{\gamma}^2)\pi\Delta\tau\theta(x).$$

In the limit as $\Delta \to 0$, (37) reduces to the normal-metal expression (9). This result has already been mentioned in the Introduction and is in fact quite natural to expect: at large frequency shifts the scattering in a superconductor does not differ from that in a normal metal. The transition to the normal metal case depends on the relation between Δ and τ^{-1}. Using (39) gives

$$-\mathrm{Im}\, K^R = \nu(\overline{\gamma^2} - \bar{\gamma}^2)x\tau\left(1 + 2\frac{\Delta}{x}\right) \tag{40}$$

for $2\Delta \ll x \ll \tau^{-1}$ and

$$-\mathrm{Im}\, K^R = \nu(\overline{\gamma^2} - \bar{\gamma}^2)\left(\frac{1}{x\tau} + 2\pi\frac{\Delta^2}{x^2}\right) \tag{41}$$

for $\tau^{-1} \ll 2\Delta \ll x$.

In the latter case, it is seen that the superconducting contribution is smaller than the normal term only for $x \gg 2\pi\Delta^2\tau$.

From Eqs. (19) and (37)–(41), the light scattering cross section may be obtained. The integral in (19) is

$$J = -\mathrm{Im}\, K^R \frac{c}{\omega_i(\varkappa_i + \varkappa_s)}.$$

The variation of the cross section with ω_0 for the limiting cases (40) and (41) is shown in Fig. 5.

I would like to thank Yu. N. Ovchinnikov and G. M. Éliashberg for helpful discussions.

The work is supported by a grant from the American Physical Society.

[1]A. A. Abrikosov and L. A. Falkovsky, Zh. Eksp. Teor. Fiz. **40**, 263 (1961) [Sov. Phys. JETP **13**, 179 (1961)].
[2]A. A. Abrikosov and L. A. Falkovsky, Physica C: Solid State Phys. **156**, 1 (1988).
[3]R. Hackl, R. Kaiser, and S. Schictanz, J. Phys. **16**, 1729 (1983).
[4]S. B. Dierker, M. B. Klein, J. W. Webb, and Z. Fisk, Phys. Rev. Lett. **50**, 853 (1983).
[5]C. Thomsen and M. Cardona, *Physical Properties of High Temperature Semiconductors* (ed. by D. M. Ginsberg), World Sci. Publ., Singapore (1989), Vol. 1, p. 409.
[6]M. Boekholt, M. Hoffmann, and G. Guentherodt, Physica C: Solid State Phys. **175**, 42 (1991).
[7]T. Staufer, R. Nemetschek, R. Hackl, P. Müller, and H. Veith, Phys. Rev. Lett. **68**, 1069 (1992).
[8]L. A. Falkovsky and S. Klama, Physica C: Solid State Phys. **172**, 242 (1990).
[9]A. A. Abrikosov, Physica C: Solid State Phys. **182**, 191 (1991).
[10]L. A. Falkovsky, Zh. Eksp. Teor. Fiz. **95**, 1146 (1989) [Sov. Phys. JETP **68**, 661 (1989)].
[11]A. Zawadowski and M. Cardona, Phys. Rev. B **42**, 10732 (1990).
[12]A. A. Abrikosov and V. M. Genkin, Zh. Eksp. Teor. Fiz. **65**, 842 (1973) [Sov. Phys. JETP **38**, 417 (1974)].
[13]L. A. Falkovsky, Zh. Eksp. Teor. Fiz. **100**, 2045 (1991) [Sov. Phys. JETP **73**, 1134 (1991)].
[14]A. A. Abrikosov, L. P. Gor'kov, and I. E. Dzyaloshinskiĭ, *Quantum Field Theoretical Methods in Statistical Physics*, Nauka, Moscow (1962) [Engl. transl. Pergamon, Oxford (1965)].

Translated by E. Strelchenko